Synthesis and Discovery of N-Carbonylpyrrolidine- or N-Sulfonylpyrrolidine-Containing Uracil Derivatives as Potent Human Deoxyuridine Triphosphatase Inhibitors

Hitoshi Miyakoshi,[†,§] Seiji Miyahara,[†,‡] Tatsushi Yokogawa,[†] Khoon Tee Chong,[†] Junko Taguchi,[†] Kanji Endoh,[†] Wakako Yano,[†] Takeshi Wakasa,[†] Hiroyuki Ueno,[†] Yayoi Takao,[†] Makoto Nomura,[†] Satoshi Shuto,[‡] Hideko Nagasawa,[§] and Masayoshi Fukuoka*,[†]

[†]Drug Discovery Research Center, Taiho Pharmaceutical Co. Ltd., Okubo 3, Tsukuba, Ibaraki 300-2611, Japan
[‡]Faculty of Pharmaceutical Sciences, Hokkaido University, Kita-12, Nishi-6, Kita-ku, Sapporo 060-0812, Japan
[§]Laboratory of Pharmaceutical and Medicinal Chemistry, Gifu Pharmaceutical University, 1-25-4 Daigaku-nishi, Gifu 501-1196, Japan

Ⓢ *Supporting Information*

ABSTRACT: Recently, deoxyuridine triphosphatase (dUT-Pase) has emerged as a potential target for drug development as part of a new strategy of 5-fluorouracil-based combination chemotherapy. We have initiated a program to develop potent drug-like dUTPase inhibitors based on structure–activity relationship (SAR) studies of uracil derivatives. N-Carbonyl-pyrrolidine- and N-sulfonylpyrrolidine-containing uracils were found to be promising scaffolds that led us to human dUTPase inhibitors (12k) having excellent potencies (IC$_{50}$ = 0.15 μM). The X-ray structure of a complex of 16a and human dUTPase revealed a unique binding mode wherein its uracil ring and phenyl ring occupy a uracil recognition region and a hydrophobic region, respectively, and are stacked on each other. Compounds 12a and 16a markedly enhanced the growth inhibition activity of 5-fluoro-2′-deoxyuridine against HeLa S3 cells in vitro (EC$_{50}$ = 0.27−0.30 μM), suggesting that our novel dUTPase inhibitors could contribute to the development of chemotherapeutic strategies when used in combination with TS inhibitors.

16a: human dUTPase
IC$_{50}$ = 0.32 μM
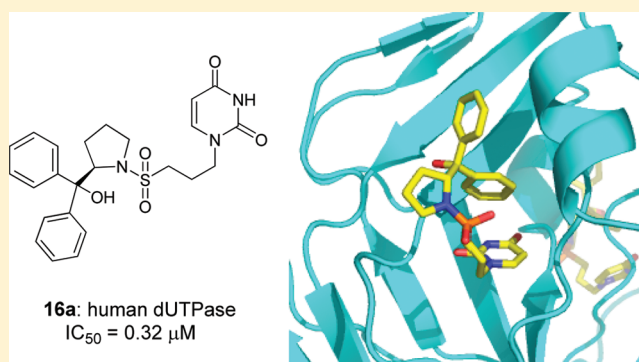
INTRODUCTION

Thymidylate synthase (TS) inhibitors,[1−3] including 5-fluorouracil (5-FU) and its derivatives, are widely used in the treatment of a range of cancers. However, the clinical antitumor effect of TS inhibitors is often restricted by the occurrence of intrinsic or acquired drug resistance. Some reports have shown that the effect of TS inhibitors can be influenced by a number of factors.[4−7] For example, Ladner et al. found that deoxyuridine triphosphatase (dUTPase, EC 3.6.1.23) could be an important determinant for the antitumor effect of TS inhibitors.[8]

TS inhibitors decrease the intracellular dTTP (thymidine triphosphate) pools (thymineless death) concurrently with increasing the deoxyuridine monophosphate (dUMP) pools, which results in expansion of intracellular deoxyuridine triphosphate (dUTP) pools. dUTP is one of the noncanonical nucleoside triphosphates (NTPs) which cause DNA damage by being incorporated into DNA.[9] Because DNA polymerase cannot recognize the difference between dTTP and dUTP,[10] the expansion of dUTP pools causes uracil misincorporation into DNA, which is one of the key mechanisms of the cytotoxity induced by TS inhibitors.[11−13] dUTPase specifically recognizes dUTP among natural NTPs and hydrolyzes it to

dUMP and pyrophosphate.[14−16] This enzyme is thought to be responsible for two biological roles: (1) decreasing the intracellular dUTP pools to prevent the uracil misincorporation instead of thymine into DNA and (2) supplying dUMP as a substrate for TS to be converted to thymidine monophosphate (dTMP), an essential precursor for the de novo pathway of DNA synthesis.[17] Therefore, dUTPase plays an important role in maintenance of the nucleotide homeostasis by strict regulation of the cellular dUTP/dTTP ratio during DNA replication and repair. In addition, it has been reported that dUTPase is also able to hydrolyze 5-fluoro-2′-deoxyuridine triphosphate (FdUTP).[18] Accordingly, dUTPase expression can mediate resistance to 5-FU by preventing the misincorporation of FdUTP and dUTP into DNA in cancer cells (Figure 1).[19−21] Indeed, siRNA-mediated suppression of human dUTPase significantly enhanced cell growth inhibition effect of 5-fluoro-2′-deoxyuridine (FdUrd) against colon and breast cancer cell lines.[22] It also has been reported that low intratumoral levels of nuclear dUTPase expression in clinical specimens are associated
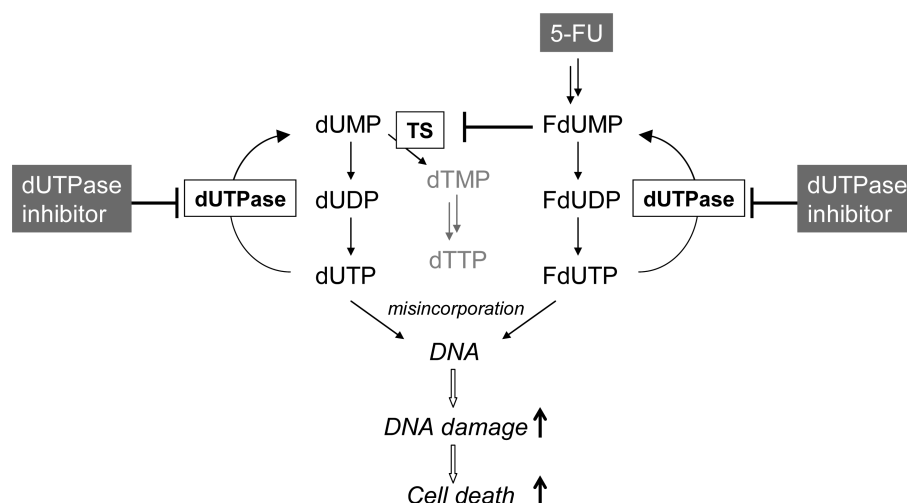
Figure 1. Proposed mechanism of the enhancing effect of dUTPase inhibitors for the antitumor effect of TS inhibitors by inducing severe DNA damage.
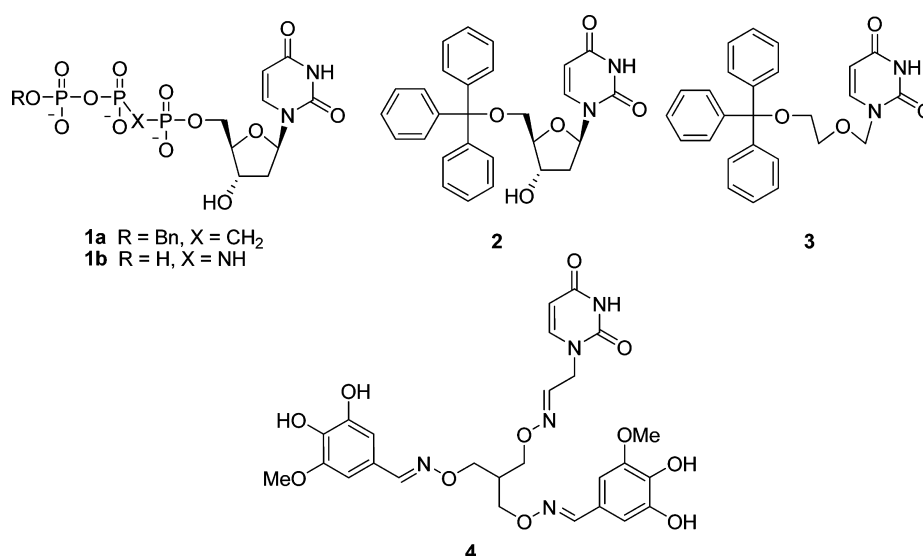

Figure 2. Structural formula of dUTPase inhibitors.

with better response to 5-FU-based chemotherapy, longer time to progression, and greater survival in colorectal cancer.[8] Furthermore, Takatori et al. have reported that nuclear dUTPase activation significantly correlates with a poor prognosis in hepatocellular carcinoma patients,[23] and Kawahara et al. also have reported that the expression of dUTPase may predict the metastatic potential of colorectal cancer.[24] Consequently, dUTPase has emerged as a potential target for chemotherapeutic drug development.

Although several previous efforts have been made to develop dUTPase inhibitors (Figure 2),[25−34] to the best of our knowledge, none of them is evaluated in clinical trials. In our own research, we focused on the specificity of the uracil ring for dUTPase and prepared a library of uracil derivatives to be screened as potential inhibitors. We then focused on compounds obtained from the first screening to develop potent drug-like dUTPase inhibitors. Such dUTPase inhibitors would provide a new strategy for combination chemotherapy with TS inhibitors. In this paper, we report the design and synthesis of novel uracil compounds, their evaluation as human dUTPase inhibitors, and their abilities to enhance the growth inhibition

activity of FdUrd against cancer cells. We also discuss the mechanism of inhibition of these new inhibitors based on X-ray analysis of the crystal structure of a complex of the dUTPase inhibitor and human dUTPase.
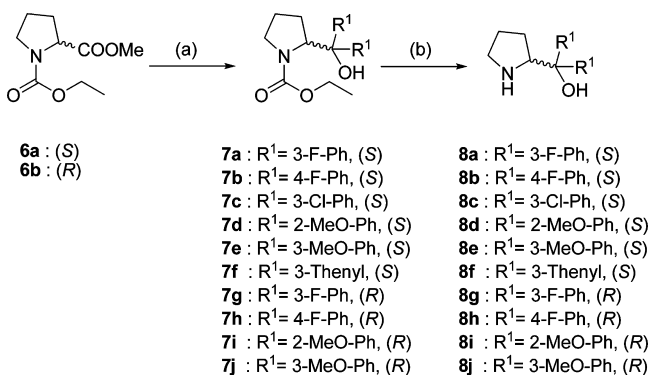
■ CHEMISTRY

Pyrrolidine derivatives **8a−j** were synthesized according to the method of Li et al.[35] In brief, chiral *N*-carboethoxy-proline methyl esters **6a** and **6b** were treated with the appropriate Grignard reagents to provide **7a−j**. These were then converted to the corresponding amines **8a−j** by removal of the ethoxycarbonyl group (Scheme 1).

Amide-containing uracil derivatives **11a−w** and *N*-carbonylpyrrolidine-containing uracil derivatives **12a−l** were prepared by a condensation reaction between a known carboxylic acid **9**[36] or **10**[36] and the appropriate amine (**8a−f**, or a known amine) (Scheme 2).

The synthesis of *N*-sulfonylpyrrolidine-containing uracil derivatives **16a−f** is shown in Scheme 3. Pyrrolidine derivatives **8g−l** were treated with 3-chloropropanesulfonyl chloride to provide **13a−f**, followed by reaction with AcONa to give **14a−f**.

Scheme 1. General Synthetic Method for Preparation of Pyrrolidine Derivatives 8a–j[a]
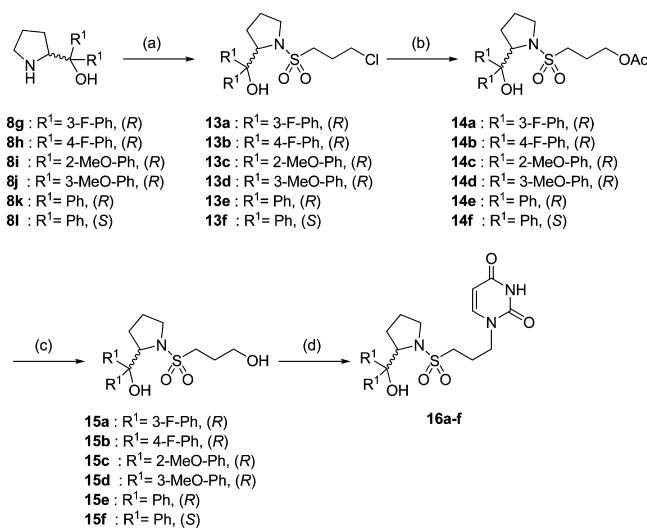

6a : (S)
6b : (R)

7a : R[1]= 3-F-Ph, (S)   8a : R[1]= 3-F-Ph, (S)
7b : R[1]= 4-F-Ph, (S)   8b : R[1]= 4-F-Ph, (S)
7c : R[1]= 3-Cl-Ph, (S)   8c : R[1]= 3-Cl-Ph, (S)
7d : R[1]= 2-MeO-Ph, (S)   8d : R[1]= 2-MeO-Ph, (S)
7e : R[1]= 3-MeO-Ph, (S)   8e : R[1]= 3-MeO-Ph, (S)
7f : R[1]= 3-Thenyl, (S)   8f : R[1]= 3-Thenyl, (S)
7g : R[1]= 3-F-Ph, (R)   8g : R[1]= 3-F-Ph, (R)
7h : R[1]= 4-F-Ph, (R)   8h : R[1]= 4-F-Ph, (R)
7i : R[1]= 2-MeO-Ph, (R)   8i : R[1]= 2-MeO-Ph, (R)
7j : R[1]= 3-MeO-Ph, (R)   8j : R[1]= 3-MeO-Ph, (R)

[a]Reagents and conditions: (a) R[1] MgBr, THF, 0 °C, 3 h, 60–81%; (b) KOH, MeOH, reflux, 12 h, 85–97%.

Scheme 2. General Synthetic Method for the Preparation of Derivatives 5 and 11a–w (See Table 1) and 12a–l (See Table 2)[a]

9: n = 1
10: n = 2

5, 11a-w   12a-l
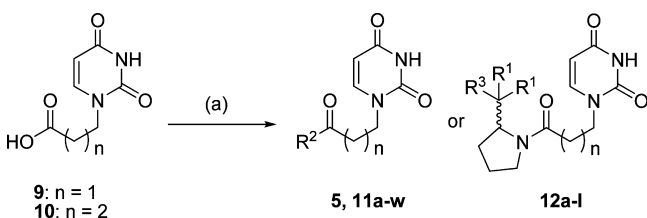
[a]Reagents and conditions: (a) amine, EDC·HCl, HOBt, DMF, room temp, 3 h, 14%–quant. R[2]: various amino groups. R[3]: H or OH.

Scheme 3. General Synthetic Method for the Preparation of Derivatives 16a–f (See Table 3)[a]

8g : R[1]= 3-F-Ph, (R)   13a : R[1]= 3-F-Ph, (R)   14a : R[1]= 3-F-Ph, (R)
8h : R[1]= 4-F-Ph, (R)   13b : R[1]= 4-F-Ph, (R)   14b : R[1]= 4-F-Ph, (R)
8i : R[1]= 2-MeO-Ph, (R)   13c : R[1]= 2-MeO-Ph, (R)   14c : R[1]= 2-MeO-Ph, (R)
8j : R[1]= 3-MeO-Ph, (R)   13d : R[1]= 3-MeO-Ph, (R)   14d : R[1]= 3-MeO-Ph, (R)
8k : R[1]= Ph, (R)   13e : R[1]= Ph, (R)   14e : R[1]= Ph, (R)
8l : R[1]= Ph, (S)   13f : R[1]= Ph, (S)   14f : R[1]= Ph, (S)

15a : R[1]= 3-F-Ph, (R)
15b : R[1]= 4-F-Ph, (R)
15c : R[1]= 2-MeO-Ph, (R)
15d : R[1]= 3-MeO-Ph, (R)
15e : R[1]= Ph, (R)
15f : R[1]= Ph, (S)

16a-f

[a]Reagents and conditions: (a) Cl(CH₂)₃SO₂Cl, TEA, CH₂Cl₂, room temp, 2 h, 73%–quant; (b) AcONa, NaI, DMF, 90 °C, 12 h, 63–70%; (c) MeNH₂, MeOH, room temp, 1 h, 92–99%; (d) N-3-Bz-uracil, PPh₃, DIAD, THF, room temp, 2 h then MeNH₂, MeOH, room temp, 1 h, 55–73%.

After removal of the acetyl group, alcohol compounds 15a–f were coupled with 3-N-benzoyluracil[37] by a Mitsunobu reaction. Removal of the benzoyl group with methylamine provided 16a–f.

RESULTS AND DISCUSSION

Molecular Design of dUTPase Inhibitors. First, we addressed the strict substrate specificity of dUTPase[14] for uracil by preparing our own library of uracil derivatives for screening as dUTPase inhibitors. In this library, we identified a hit compound 5 (IC$_{50}$ = 97 μM) which had moderate but superior or comparable inhibitory activity to those of the known dUTPase inhibitors such as 1b and 3 (Table 1). This finding enforced us to perform further structure–activity relationship (SAR) studies focused on amide or sulfonamide-containing uracil structures in which the linker and amine moiety of hit compound 5 were modified for structural optimization to improve inhibitory potency (Figure 3).
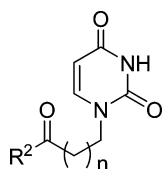
Structure–Activity Relationship Study of Amide-Containing Uracil Derivatives. Human dUTPase inhibitory activities of amide-containing uracil derivatives are shown in Table 1. Among the derivatives having an ethylene linker (n = 1), 11i (IC$_{50}$ = 7.3 μM) showed an almost 2-fold greater potency as a dUTPase inhibitor compared to the substrate dUTP-mimic 1b. Among the derivatives having a trimethylene linker (n = 2), 11q (IC$_{50}$ =16 μM) and 11r (IC$_{50}$ = 2.5 μM) having the N-2,2-diphenylethyl moiety possessed moderate potencies. In particular, 11s (IC$_{50}$ = 1.3 μM) and 11w (IC$_{50}$ = 1.1 μM), bearing both a diphenylmethyl and a tert-amide group, have relatively high and comparable potency that is not influenced by the presence or absence of the tert-alcohol group. These derivatives also have a favorable level of lipophilicity (clogP: 1.83–2.17).

SAR study of these amide-containing uracil derivatives showed clearly that the tert-amide compound 11s had almost a 12-fold more potent inhibitory activity compared to the sec-amide compound 11q. Interestingly, the ¹H NMR spectrum and NOE data of 11s in DMSO-d$_6$ revealed that 11s existed as mixture of two conformational isomers at 25 °C (cis:trans = 2:3) (Figure 4, see also Figure S1 in the Supporting Information). Although it is not apparent, the existence of the cis-isomer of tert-amide 11s may make some contribution to binding to the enzyme. We may suppose that the extra hydrophobic interaction of the tert-amide methyl group could be the key to its higher activity.

Structure–Activity Relationship Study of N-Carbonylpyrrolidine-Containing Uracil Derivatives. Next, we envisaged that reducing the entropy loss associated with binding of the bulky alkyl amino chain present in 11s could increase binding to the enzyme and translate into increased inhibitory activity. On the basis of this hypothesis, we designed and synthesized N-carbonylpyrrolidine-containing uracil derivatives that have enhanced rigidity of the side chain relative to 11s because of the reduced number of rotatable bonds.

We were pleased that our prediction proved to be correct. In fact, certain of the N-carbonylpyrrolidine derivatives had remarkably increased inhibitory activity. This structural adjustment also resulted in a more favorable level of lipophilicity (Table 2). A comparison of the potency of 12a (S configuration) to that of 12b (R configuration) revealed the influence of the stereochemistry at the C-2 position of the pyrrolidine ring. Thus, the S enantiomer, 12a, was a highly potent inhibitor (IC$_{50}$ = 0.29 μM). By comparison, the potency of 12b (R configuration, IC$_{50}$ = 10 μM, eudismic ratio = 34) was significantly weaker than that of 12a. On the basis of this result, various derivatives having the S configuration were synthesized for evaluation. Compound 12k, wherein the hydroxyl group is absent, also had higher potency than 12a. This result clearly suggests that the terminal hydroxyl

Table 1. Human dUTPase Inhibitory Activity of Amide-Containing Uracil Derivatives 5, 11a−w, and Reference Compounds 1−4

	n	R²	clogP[a]	IC50 (µM)[b]
1a			-4.23	N.T. (Ki = 0.3 µM)[c]
1b			-6.52	15±1.4 (Ki = 5 µM)[c]
2			4.46	N.T. (Ki = 18 µM)[c]
3			4.96	>300 (Ki = 17 µM)[c]
4			3.16	N.T. (IC_{50} = 3.3 µM)[c]
5	2	-NHC(CH3)3	-0.71	97±2.0
11a	1	-NHC(CH3)2CH2C(CH3)3	0.83	>30
11b	1	-NHC(CH2CH3)3	0.67	22±0.59
11c	1	-NHC(CH3)3	-0.93	>30
11d	1	-N(CH2Ph)2	1.65	>30
11e	1	-NHCHPh2	1.38	>30
11f	1	-NHCH2CHPh2	1.61	>30
11g	1	-NHCH2CH2CHPh2	1.98	>30
11h	1	-N◯Ph	1.62	>30
11i	1	-NHC(CH3)2C(OH)Ph2	1.75	7.3±0.32
11j	2	-NHPh	0.19	>30
11k	2	-NHC(CH3)2CH2C(CH3)3	1.05	30±0.60
11l	2	-NHCH2Ph	-0.15	>30
11m	2	-NHC(CH3)2CH2Ph	0.93	>30
11n	2	-NHC(CH3)2Ph	0.55	>30
11o	2	-NHC(CH2CH3)3	0.88	>30
11p	2	-NHCHPh2	1.60	>30
11q	2	-NHCH2CHPh2	1.83	16±0.39
11r	2	-NHC(CH3)2C(OH)Ph2	1.96	2.5±0.071
11s	2	-N(CH3)CH2CHPh2	2.17	1.3±0.068
11t	2	-N̄ (naphthylmethyl)	2.16	>30
11u	2	-NHC(CH3)2(CH2)2Ph	1.38	21±0.72
11v	2	-NHC(CH3)2CH2OH	-1.82	>30
11w	2	-N(CH3)CH2C(OH)Ph2	1.87	1.1±0.038

[a]See Experimental Section. [b]Except compounds **1a−b**, **2−3**, and **5**, enzyme inhibition assay are tested at 30 µM or below. IC_{50} values are shown as the mean ± SE (n = 3). [c]Reference data **1a**,[25] **1b**,[26] **2**,[27] **3**,[29] and **4**.[30] N.T. = not tested

group of *N*-carbonylpyrrolidine-containing uracil derivatives does not contribute to their potency as dUTPase inhibitors. These studies also revealed that the trimethylene linker (n = 2) between the uracil ring and carbonyl moiety of the amide group is better
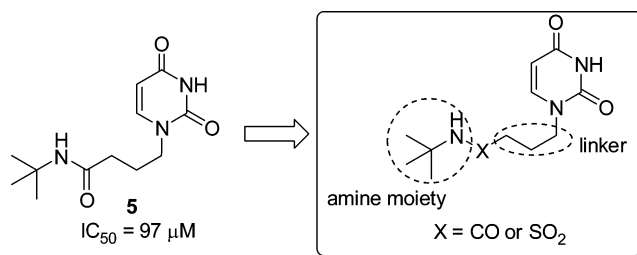

Figure 3. Structural formula of hit compound **5** (X = CO) and molecular modification for the SAR study.

than an ethylene linker (n = 1) because the potency of **12l** bearing an ethylene linker was much less than that of **12a**.

We next evaluated the effect of aromatic substituents R² on potency by comparing the activities of compounds **12c−j** to **12a**. Although the inhibitory activities of the analogues with electron-withdrawing groups such as F and Cl on the phenyl ring were comparable to that of **12a**, the parent compound **12a** remained the best activity, while introduction of a electron-donating methoxy group into any position of the terminal phenyl ring obviously lowered inhibitory activity (**12g−i**). The thiophenyl isosteric isomer **12j** was as potent as the parent **12a**.

Structure−Activity Relationship Study of *N*-Sulfonyl-pyrrolidine-Containing Uracil Derivatives. We also designed and synthesized several *N*-sulfonylpyrrolidine-containing uracil derivatives to examine the effects of structural changes in the sulfonamide series (Table 3). It is interesting that, in a series of sulfonamide derivatives, the R enantiomer (**16a**) was a significantly more potent inhibitor of dUTPase (IC_{50} = 0.32 µM) than the corresponding S enantiomer (**16b**; IC_{50} = 9.4 µM, eudismic ratio = 29), in contrast to the *N*-carbonylpyrrolidine-containing uracil series. Introduction of a fluorine atom into the *m*- or *p*-position of the terminal phenyl ring of **16a** did not diminish the highly potent inhibitory activity (**16c−d**, IC_{50} =0.28−0.31 µM). However, introduction of a methoxy group into the *o*- or *m*-position clearly reduced potency, similar to the results observed with the *N*-carbonylpyrrolidine derivatives.

The strategies describe above have allowed us to develop highly potent dUTPase inhibitors *N*-carbonylpyrrolidine-containing uracil derivatives such as **12a** (IC_{50} = 0.29 µM) and *N*-sulfonylpyrrolidine-containing derivatives such as **16a** (IC_{50} = 0.32 µM). In particular, the most potent compound, **12k** (IC_{50} = 0.15 µM), was a remarkably more potent inhibitor of dUTPase (ca. 100−2000-fold) than previously described dUTPase inhibitors such as compounds **1−3**. These novel dUTPase inhibitors also have drug-like properties that meet the standards of Lipinsky's rule-of-five (for example: **12a** clogP, 1.82; molecular weight, 433.5; H-bond donors, 2; H-bond acceptors, 7; **16a** clogP, 1.92; molecular weight, 469.6; H-bond donors, 2; H-bond acceptors, 8).[38] Among previously described dUTPase inhibitors, compound **4** was reported to be the most potent.[30] However, **4** does not satisfy Lipinsky's rule-of-five (molecular weight, 587.54 >500; H-bond acceptors, 16 >10).

Human dUTPase Inhibitors Enhances Growth Inhibition Activity of FdUrd in Vitro. We performed in vitro growth inhibition experiments with certain of our novel dUTPase inhibitors. These studies were done on HeLa S3 cells in combination with FdUrd to evaluate the chemotherapeutic enhancing effects of the dUTPase inhibitors. We performed cell proliferation assay by treatment with FdUrd at the concentration of 1 µM combined with various concentrations of the dUTPase inhibitor. T/C (%) value was obtained as the ratio of cell density determined
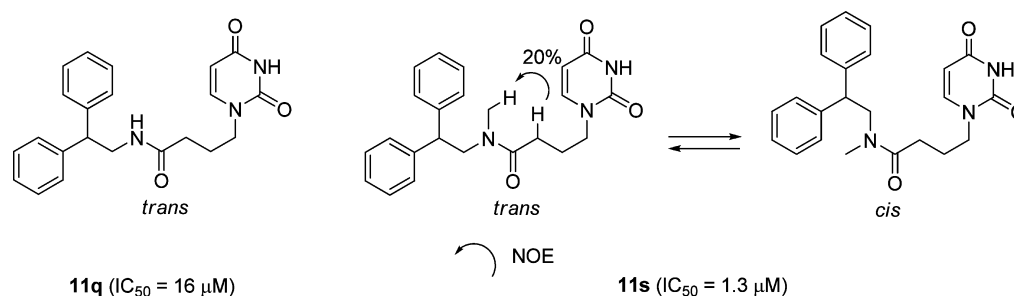
Figure 4. Conformational preference of amide compounds **11q** (*trans*) and **11s** (*trans* and *cis*).

Table 2. Human dUTPase Inhibitory Activity of *N*-Carbonylpyrrolidine-Containing Uracil Derivatives 12a–l and 11s

	n	S or R	R^2	R^3	clogP[a]	IC$_{50}$ (μM)[b]
11s					2.17	1.3 ± 0.068
12a	2	S	Ph	OH	1.82	0.29 ± 0.015
12b	2	R	Ph	OH	1.82	10 ± 0.30
12c	2	S	3-F-Ph	OH	1.92	0.35 ± 0.017
12d	2	S	4-F-Ph	OH	1.92	0.60 ± 0.014
12e	2	S	3-Cl-Ph	OH	3.01	0.58 ± 0.027
12f	2	S	4-Cl-Ph	OH	3.01	>1.0[c]
12g	2	S	2-MeO-Ph	OH	1.65	>1.0[c]
12h	2	S	3-MeO-Ph	OH	1.65	>1.0[c]
12i	2	S	4-MeO-Ph	OH	1.65	>1.0[c]
12j	2	S	3-thienyl	OH	1.17	0.23 ± 0.0033
12k	2	S	Ph	H	2.81	0.15 ± 0.0094
12l	1	S	Ph	OH	1.60	>1.0[c]

[a]See Experimental Section. [b]IC$_{50}$ values are shown as the mean ± SE ($n = 3$). [c]Except **12b**, enzyme inhibition assay are tested at 1.0 μM or below.

Table 3. Human dUTPase Inhibitory Activity of *N*-Sulfonylpyrrolidine-Containing Uracil Derivatives 16a–f and 11s

	S or R	R^2	clogP[a]	IC$_{50}$ (μM)[b]
11s			2.17	1.3 ± 0.068
16a	R	Ph	1.92	0.32 ± 0.018
16b	S	Ph	1.92	9.4 ± 0.085
16c	R	3-F-Ph	2.02	0.28 ± 0.0026
16d	R	4-F-Ph	2.02	0.31 ± 0.0071
16e	R	2-MeO-Ph	1.75	>1.0[c]
16f	R	3-MeO-Ph	1.75	>1.0[c]

[a]See Experimental Section. [b]IC$_{50}$ values are shown as the mean ± SE ($n = 3$). [c]Except **16b**, enzyme inhibition assay are tested at 1.0 μM or below.

by the Crystal Violet assay with drug treatment to without drug treatment for 24 h. To show the enhancement effect of the dUTPase inhibitor for growth inhibition activity of FdUrd, EC$_{50}$ (μM) value was calculated from concentration-T/C (%) curve as the concentration reducing by half the T/C (%) value by treatment with only FdUrd (T/C 70–80%).

We chose four representative compounds (**11r**, **11s**, **12a**, and **16a**) from each derivative reported in this paper (Table 4).

Table 4. The Enhancing Effect of dUTPase Inhibitors for Growth Inhibition Activity of FdUrd against HeLa S3 Cells in Vitro

	cytotoxicity EC$_{50}$ (μM)[a]	EC$_{50}$ (μM) with 1 μM FdUrd[b]	dUTPase IC$_{50}$ (μM)[c]
11r	>100	3.0 ± 0.10	2.5 ± 0.071
11s	>100	1.2 ± 0.037	1.3 ± 0.068
12a	>100	0.27 ± 0.0041	0.29 ± 0.015
16a	>100	0.30 ± 0.0050	0.32 ± 0.018

[a]Cytotoxity of dUTPase inhibitors against HeLa S3 cells (72 h). [b]EC$_{50}$ value shows the concentration at which the dUTPase inhibitor reduces by half the T/C (%) value of FdUrd (1 μM, 70–80%) against HeLa S3 cells (24 h). EC$_{50}$ values are shown as the mean ± SE ($n = 3$). [c]IC$_{50}$ value shows dUTPase inhibitory activity as the mean ± SE ($n = 3$).

None of the compounds inhibited growth of HeLa S3 cells by themselves at the concentration of 100 μM for 72 h. However, low concentration of each of these compounds dramatically enhanced the FdUrd (1 μM) mediated inhibition of growth of HeLa S3 (EC$_{50}$ = 0.27–3.0 μM). Moreover, the degree of the enhancement correlated well with the potency of dUTPase inhibition. On the basis of these results, the ability of these compounds to enhance the growth inhibition mediated by FdUrd clearly can be ascribed to their ability to inhibit dUTPase in HeLa S3 cells.

X-Ray Structure of a Complex of 16a and dUTPase. Our novel dUTPase inhibitors that possess a uracil ring and either a chiral diphenylmethyl pyrrolidylamide or sulfonamide moiety are quite different in structure from the natural substrate dUTP. Nevertheless, they are highly potent inhibitors of dUTPase, suggesting that the active site of the enzyme can recognize these structures as readily as dUTP (the concentration of a substrate dUTP in the enzyme inhibition assays is 0.1 μM). Therefore, elucidation of the binding mode of these derivatives to the active site of dUTPase by using X-ray diffraction data should facilitate development of additional potent inhibitors for clinical use. Accordingly, high-resolution data (1.7 Å) was obtained from a cocrystal of human dUTPase with the highly potent *N*-sulfonylpyrrolidine containing inhibitor **16a**. This allowed the visualization of the electron density map

of the enzyme—inhibitor complex. A summary of statistics for data collection and refinement are shown in Table S1 in the Supporting Information.

Figure 5A shows the principal polar interactions between human dUTPase and **16a** in the cocrystal structure. The
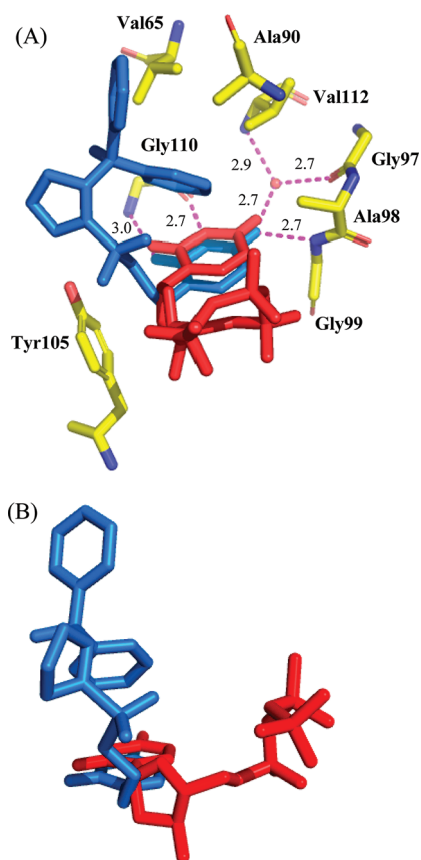

Figure 5. Binding of **16a** (blue stick) in the catalytic site of human dUTPase. (A) Polar interactions. Distances [Å] are indicated. Waters are shown as small spheres. Red stick depicted α,β-imino dUTP **1b** in the human dUTPase:α,β-imino dUTP **1b** structure (PDB code: 2HQU)[39] superimposed on the **16a**:human dUTPase. (B) Comparison of **16a** (blue stick) with α,β-imino dUTP **1b** (red stick).

structure of α,β-imino dUTP **1b** in human dUTPase:α,β-imino dUTP **1b** complex (PDB code: 2HQU)[39] is also superimposed on the cocrystal structure of human dUTPase and **16a**. It is interesting to note that this superimposition reveals very little overlap between **1b** and **16a**. Only the uracil rings overlap closely, occupying the uracil recognition region of the enzyme (Figure 5B). These data also reveal that the sulfonamide and diphenylmethanol moieties of **16a** do not interact with the amino acid residues that recognize the sugar and triphosphate moieties of **1b**. Furthermore, one of the terminal phenyl rings of **16a** is located in a hydrophobic region, formed by Val65, Ala90, Ala98, and Val112 residues of the enzyme, and is stacked with its own uracil ring in the active site of the enzyme. Figure 5B clearly shows that the orientation of **16a** bound to the enzyme is different from that of the substrate dUTP mimic **1b**.

Superimposition of **16a** in the cocrystal structure of human dUTPase and **16a** on the X-ray structure of α,β-imino-dUTP **1b** in the active site of dUTPase is shown in Figure 6. It is known that the flexible C-terminal tails of the third subunit of trimeric dUTPase, which are disordered in the uncomplexed
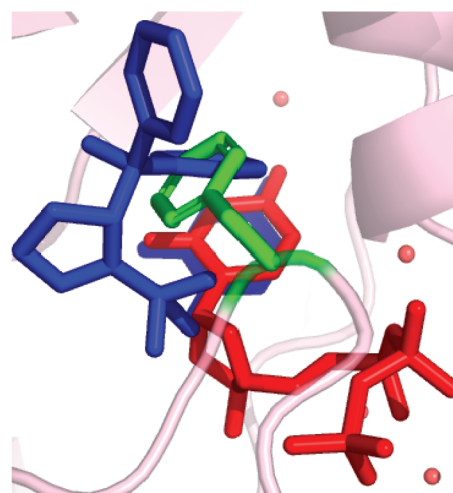

Figure 6. Superimposition of **16a** (blue stick) on the catalytic site of X-ray structure of dUTPase (light-pink ribon) with α,β-imino-dUTP **1b** (red stick) (PDB code: 2HQU).[39] The green residue is Phe158 of a C-terminal tail. Ordering of the C-terminal tails upon the active sites is essential for initiation of dUTPase catalysis.[14,39]

structure, become ordered upon ligand binding to each of the active sites between two subunits. The ordering of the C-terminal tails is essential for the trimeric dUTPase enzyme to exhibit enzymatic function.[14,39] In detail, the phenyl ring of Phe158 in this flexible tail is located in a hydrophobic region formed by Val65, Ala90, Ala98, and Val112 and is stacked with the uracil ring of a substrate. This stacking interaction is essential for dUTPase catalysis. Details of Figures 5A and 6 suggest that one of the terminal phenyl rings of **16a** occupies the hydrophobic region instead of the phenyl ring of Phe158. It follows that the potency of **16a** as a dUTPase inhibitor may be attributed to this stable interaction between its phenyl ring and the hydrophobic region of the catalytic pocket, an interaction that inhibits the ordering the C-terminal tails required for enzyme activation.

The Effects of Stereochemistry at C-2 Position of Pyrrolidine Ring of *N*-Sulfonylpyrrolidine-Containing Uracil Derivatives on Human dUTPase Inhibition Activity. SAR studies for *N*-carbonylpyrrolidine-containing uracil derivatives and *N*-sulfonylpyrrolidine-containing uracil derivatives suggest that the stereochemistry at C-2 position of their pyrrolidine rings markedly influences their potencies as inhibitors of dUTPase. Initially, we tried to evaluate the effect of streochemistry on the potency of enzyme inhibition activity by docking studies with dUTPase-enantiomeric sulfonamide inhibitors **16a** (*R*) and **16b** (*S*) based on the X-ray cocrystal structure of human dUTPase and **16a**. However, the order of the derived factors of contact surface areas of **16a** and **16b** with human dUTPase (**16a**, 565.5 Å^2; **16b**, 590.9 Å^2) proved to be opposite from what would be expected from their observed relative potencies (**16a**, 0.32 μM; **16b**, 9.4 μM). (see Figure S2 in the Supporting Information). We next considered the position of pyrrolidine ring of **16a** in the active site of dUTPase. Tyr105 is a critical residue that discriminates between the 2′-deoxyribose moiety of a substrate dUTP from the ribose moiety of UTP. The rigidity of the Tyr105 position is one of the pivotal factors that contribute to the narrow substrate specificity of dUTPase.[14] This rigidity is sustained by hydrogen bonding between the phenol group of Tyr105 and carbonyl group of Asn108. However, this hydrogen bond faces the solvent region

and is exposed to surrounding water. Fernandez et al. proposed that the hydrophobic groups of ligands would exclude surrounding water from the peripheral region of the hydrogen bond, which plays a pivotal role for the catalytic functions by a structural maintenance (wrapping) effect to stabilize a ligand–enzyme complex.[40–42] The X-ray structure of **16a** suggests that its pyrrolidine ring is proximal to Tyr105 and stabilizes a ligand–enzyme complex by removing water molecules (wrapping) from the peripheral region of Tyr105–Asn108 pair (Figure 7). In contrast, the binding model of **16b** indicates
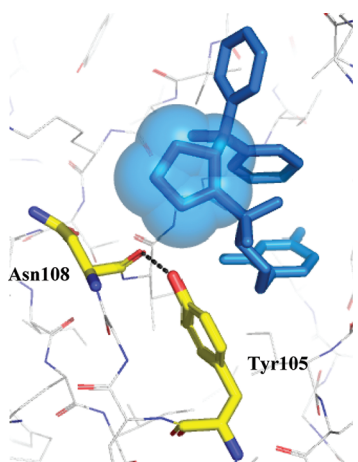

Figure 7. X-ray structure of **16a** (blue stick and sphere) in the catalytic site of dUTPase. The pyrrolidine group of **16a** likely excludes surrounding water from the backbone hydrogen bond (Tyr105–Asn108).

that its pyrrolidine ring is not found in the neighborhood of the Tyr105–Asn108 pair. Therefore, **16b** cannot induce a wrapping effect of the Tyr105–Asn108 pair (see Figure S2 in the Supporting Information). These considerations suggest that the greater potency of **16a** compared to **16b** can be attributed to stabilization of the **16a**–enzyme complex by dehydration of the peripheral region of Tyr105–Asn108 pair that is covered by the pyrrolidine ring of **16a** in the complex. In the case of *N*-carbonylpyrrolidine derivatives **12a** and **12b**, because we could not solve their X-ray crystal structures with human dUTPase and amide structure is quite different from sulfonamide, further studies are necessary to rationalize the effects of the stereo-chemistry on their inhibitory activity.

CONCLUSIONS

Using SAR studies of the linker and amine moieties of lead compound **5**, identified from preliminary screening of our own library of uracil derivatives, we identified a *tert*-amide-containing uracil derivative **11s** that is a potent inhibitor of dUTPase (IC_{50} = 1.3 μM). Further structural optimizations led to the development of the *N*-carbonylpyrrolidine-containing uracil derivatives **12a** (IC_{50} = 0.29 μM), **12k** (IC_{50} = 0.15 μM), and *N*-sulfonylpyrrolidine-containing derivative **16a** (IC_{50} = 0.32 μM), which have excellent potencies and good drug-like properties as human dUTPase inhibitors. Their inhibitory activities were markedly more potent (>1000-fold) than those of the known dUTPase inhibitors **2** and **3** which possess drug-like properties. In addition, the degree of recognition of **12k** by dUTPase was estimated to be almost comparable to that of the natural substrate dUTP because the IC_{50} values were of the same order of magnitude as that of the concentration of dUTP

(0.1 μM) in the enzyme inhibition assays. It is particularly worth noting that **12a** and **16a** markedly enhanced the growth inhibition activity of FdUrd against HeLa S3 cells at low concentrations, having EC_{50} values in the 10^{-7} M range. We also achieved crystallization of dUTPase with **16a** and obtained an X-ray analysis of the complex. The X-ray structure revealed that the high potency of **16a** can be attributed to two factors: (1) it is bound to the substrate recognition site and (2) its phenyl group occupies the hydrophobic pocket (formed by Val65, Ala90, Ala98, and Val112) and forms a stacking interaction with its own uracil. Finally, these results suggest that our novel dUTPase inhibitors should open the way to new beneficial chemotherapeutic strategies for cancer patients when used in combination with TS inhibitor.

EXPERIMENTAL SECTION

General Methods and Materials. All commercially available starting materials and solvents were reagent grade. Silica gel column chromatography was performed on Merck silica gel 60 (230–400 mesh). ^{1}H NMR spectra were measured at 270 MHz on a JEOL JNM-EX270 or 400 MHz on a JEOL JNM-LA400. ^{13}C NMR spectra were measured 100 MHz on a JEOL JNM-LA400. Chemical shifts were recorded in parts per million (ppm, δ) and were reported relative to the solvent peak or internal tetramethylsilane peak. High-resolution mass spectra (HRMS) were measured with JEOL JMS-700 (FAB) or Waters micromass Q-Tof-2 (TOF). Chemical purities of tested compounds were determined by combustion analysis or HPLC analysis and confirmed ≥95% purity. Combustion analyses (C, H, N) were performed on a Thermo Electron Corp. Flash EA 1112 series, and values were within ±0.4% of the theoretical values. Chemical purities of tested compounds **11i** and **11r** were determined by HPLC analysis with SHIMADZU Prominence HPLC system, and the values are presented in the Supporting Information. Optical rotations were measured by HORIBA SEPA-200 polarimeter. clogP values shown in Tables 1–3 were calculated ACD/LogP algorithm (ACD/Laboratories Release 10.00, version 10.01).

General Procedure for the Synthesis of 7a–7j (Method A). Exemplified for (*S*)-Ethyl 2-(Bis(3-fluorophenyl)(hydroxy)-methyl)pyrrolidine-1-carboxylate (7a). A THF solution of 3-fluorophenylmagnesium bromide (1.0 M, 20 mL, 20 mmol) was added dropwise over 5 min to a solution of *N*-carboethoxy-L-proline methyl ester **6a** (1.0 g, 5.0 mmol) in THF (30 mL) at 0 °C. After being stirred at the same temperature for 3 h, the reaction was quenched by addition of saturated aq NH_4Cl (10 mL). The separated organic phase was washed with brine (10 mL), dried over Na_2SO_4, and concentrated to dryness in vacuo. The residue was purified by a silica gel column chromatography (25–33% AcOEt in hexane) to give **7a** (1.41 g, 78%, a colorless solid). ^{1}H NMR (CDCl$_3$) δ 0.89–0.99 (1H, m), 1.24 (3H, t, *J* = 7.0 Hz), 1.50–1.63 (1H, m), 1.86–1.97 (1H, m), 2.02–2.16 (1H, m), 2.96–3.06 (1H, m), 3.41–3.51 (1H, m), 4.12–4.15 (2H, m), 4.83 (1H, dd, *J* = 4.3, 8.9 Hz), 6.94–7.09 (2H, m), 7.12–7.33 (6H, m). FAB-HRMS *m/z* [M+Na]$^+$: calcd for $C_{20}H_{21}F_2NO_3Na$, 384.1387; found, 384.1385

General Procedure for the Synthesis of 8a–8j (Method B). Exemplified for (*S*)-Bis(3-fluorophenyl)(pyrrolidin-2-yl)-methanol (8a). Potassium hydroxide (2.19 g, 39 mmol) was added to a solution of **7a** (1.41 g, 3.9 mmol) in MeOH (10 mL). The mixture was heated at reflux for 12 h. The mixture was evaporated to give a residue, which was dissolved in water (10 mL) and then extracted with CHCl$_3$ (20 mL). The organic phase was washed with water (10 mL) and brine (10 mL), dried over K_2CO_3, and concentrated in vacuo. The residue was coevaporated with toluene (10 mL × 3) to give **8a** (1.07 g, 95% as a colorless gum). ^{1}H NMR (DMSO-d_6) δ 1.36–1.45 (2H, m), 1.51–1.63 (2H, m), 2.40 (1H, brs), 2.75–2.88 (2H, m), 4.26 (1H, t, *J* = 7.6 Hz), 5.35 (1H, brs), 6.94–7.02 (2H, m), 7.25–7.45 (6H, m). FAB-HRMS *m/z* [M + H]$^+$: calcd for $C_{17}H_{18}F_2NO$, 290.1356; found, 290.1380

General Procedure for the Synthesis of 5 and 11a–11w (Method C). Exemplified for *N-tert*-Butyl-4-(2,4-dioxo-3,4-dihydropyrimidin-1(2*H*)-yl)butanamide (5). A mixture of 4-(2,4-dioxo-3,4-dihydropyrimidin-1(2*H*)-yl)butanoic acid **10**[36] (135 mg, 0.68 mmol), *tert*-butylamine (143 μL, 1.36 mmol), EDC·HCl (196 mg, 1.02 mmol), and HOBt (110 mg, 0.82 mmol) in DMF (4.0 mL) was stirred at room temperature for 3 h. The reaction mixture was evaporated, and the residue was purified by a silica gel column chromatography (1–3% MeOH in CHCl$_3$) to give **5** (34 mg, 20% as a colorless solid). ^{1}H NMR (DMSO-*d$_6$*) δ 1.21 (9H, s), 1.69–1.80 (2H, m), 2.01 (2H, t, *J* = 7.3 Hz), 3.63 (2H, t, *J* = 7.0 Hz), 5.52 (1H, dd, *J* = 2.4, 7.8 Hz), 7.39 (1H, brs), 7.57 (1H, d, *J* = 7.8 Hz), 11.18 (1H, brs). ^{13}C NMR (CDCl$_3$) δ 24.81, 28.67, 33.22, 47.70, 51.18, 102.27, 144.82, 151.44, 164.05, 170.92. Anal. Calcd for C$_{12}$H$_{19}$N$_3$O$_3$: C, 56.90; H, 7.56; N, 16.59. Found: C, 56.74; H, 7.67; N, 16.41

General Procedure for the Synthesis of 12a–l (Method D). Exemplified for (*S*)-1-(4-(2-(Hydroxydiphenylmethyl)-pyrrolidin-1-yl)-4-oxobutyl)pyrimidine-2,4(1*H*,3*H*)-dione (12a). A mixture of **10** (40 mg, 0.22 mmol), (*S*)-(−)-α,α-diphenyl-2-pyrrolidinemethanol (56 mg, 0.22 mmol), EDC·HCl (57 mg, 0.3 mmol), and HOBt (35 mg, 0.26 mmol) in DMF (2.0 mL) was stirred at room temperature for 3 h. The reaction mixture was evaporated, and the residue was purified by a silica gel column chromatography (1–3% MeOH in CHCl$_3$) to give **12a** (62 mg, 65% as a colorless foam). ^{1}H NMR (CDCl$_3$) δ 1.00–1.09 (1H, m), 1.54–1.65 (1H, m), 1.90–2.09 (4H, m), 2.19–2.40 (2H, m), 3.01–3.11 (1H, m), 3.35–3.44 (1H, m), 3.50–3.60 (1H, m), 3.67–3.77 (1H, m), 5.13 (1H, dd, *J* = 5.7, 8.4 Hz), 5.69 (1H, dd, *J* = 1.9, 7.8 Hz), 6.70 (1H, s), 7.14 (1H, d, *J* = 7.8 Hz), 7.21–7.42 (10H, m), 8.68 (1H, brs). ^{13}C NMR (CDCl$_3$) δ 23.27, 23.87, 29.80, 31.02, 47.72, 48.75, 67.39, 81.57, 102.13, 127.34, 127.40, 127.57, 127.87, 127.98, 143.52, 145.02, 146.06, 150.83, 163.54, 173.77. Anal. Calcd for C$_{25}$H$_{27}$N$_3$O$_4$·H$_2$O: C, 66.50; H, 6.47; N, 9.31. Found: C, 66.78; H, 6.11; N, 9.23; [α]$^{25}_D$ = −102.58 (*c* 1.08, CHCl$_3$)

General Procedure for the Synthesis of 13a–f (Method E). Exemplified for (*R*)-(1-(3-Chloropropylsulfonyl)pyrrolidin-2-yl)-diphenylmethanol (13e). To a solution of (*S*)-(−)-α,α-diphenyl-2-pyrrolidinemethanol **8k** (500 mg, 2.0 mmol) and triethylamine (554 μL) in CH$_2$Cl$_2$ (10 mL), was added 3-chloropropanesulfonyl chloride (287 μL, 2.4 mmol) at 0 °C, and the mixture was stirred at room temperature for 2 h. Saturated aq NaHCO$_3$ (5 mL) was added and partitioned. The organic layer was washed with water (5 mL) and brine (5 mL), dried over Na$_2$SO$_4$, and filtered. The filtrate was evaporated to give a residue, which was purified by a silica gel column chromatography (10–20% AcOEt in hexane) to give **13e** (800 mg, quant as a colorless solid). ^{1}H NMR (CDCl$_3$) δ 1.39–1.44 (1H, m), 1.66–1.77 (1H, m), 1.88–2.00 (1H, m), 2.04–2.24 (3H, m), 2.55–2.70 (2H, m), 2.94–3.03 (1H, m), 3.01 (1H, s), 3.47–3.56 (2H, m), 3.66–3.75 (1H, m), 5.28 (1H, dd, *J* = 4.1, 8.9 Hz), 7.23–7.36 (6H, m), 7.41–7.46 (2H, m), 7.50–7.54 (2H, m). FAB-HRMS *m/z* [M − H]$^-$: calcd for C$_{20}$H$_{23}$ClNO$_3$S, 392.1087; found, 392.1067

General Procedure for the Synthesis of 14a–f (Method F). Exemplified for (*R*)-3-(2-(Hydroxydiphenylmethyl)pyrrolidin-1-ylsulfonyl)propyl Acetate (14e). A mixture of **13e** (800 mg, 2.0 mmol), sodium acetate (492 mg, 6.0 mmol), and sodium iodide (300 mg, 2.0 mmol) in DMF (8 mL) was stirred at 90 °C for 12 h. The mixture was cooled to room temperature and diluted with AcOEt (10 mL) and toluene (10 mL) and then was washed with water (20 mL × 2) and brine (20 mL). The organic layer was dried over Na$_2$SO$_4$ and filtered. The filtrate was evaporated to give a residue, which was purified by a silica gel column chromatography (20–40% AcOEt in hexane) to give **14e** (584 mg, 70% as a colorless solid). ^{1}H NMR (CDCl$_3$) δ 1.41–1.48 (1H, m), 1.67–1.77 (1H, m), 1.90–1.97 (3H, m), 2.06 (3H, s), 2.16–2.23 (1H, m), 2.37–2.48 (1H, m), 2.54–2.62 (1H, m), 2.94–3.03 (1H, m), 2.99 (1H, s), 3.68–3.76 (1H, m), 4.00 (2H, t, *J* = 6.2 Hz), 5.31 (1H, dd, *J* = 3.5, 8.4 Hz), 7.22–7.35 (6H, m), 7.44 (2H, d, *J* = 7.6 Hz), 7.53 (2H, d, *J* = 8.1 Hz). FAB-HRMS *m/z* [M − H]$^-$: calcd for C$_{22}$H$_{26}$NO$_5$S, 416.1532; found, 416.1560

General Procedure for the Synthesis of 15a–f (Method G). Exemplified for (*R*)-3-(2-(Hydroxydiphenylmethyl)pyrrolidin-1-ylsulfonyl)propan-1-ol (15e). A mixture of **14e** (584 mg, 1.4 mmol) in MeOH solution of methylamine (9.8 M, 5 mL) was stirred at room

temperature for 1 h. The reaction mixture was evaporated, and the residue was purified by a silica gel column chromatography (50–75% AcOEt in hexane) to give **15e** (473 mg, 95% as a colorless solid). ^{1}H NMR (CDCl$_3$) δ 1.34–1.44 (1H, m), 1.62–1.76 (1H, m), 1.83–1.99 (3H, m), 2.12–2.26 (1H, m), 2.57 (1H, quint, *J* = 7.3 Hz), 2.69 (1H, quint, *J* = 7.3 Hz), 2.98 (1H, dt, *J* = 7.6, 10.8 Hz), 3.30 (1H, s), 3.61–3.74 (3H, m), 5.27 (1H, dd, *J* = 3.8, 8.64 Hz), 7.22–7.36 (6H, m), 7.42–7.46 (2H, m), 7.52–7.56 (2H, m). FAB-HRMS *m/z* [M − H]$^-$: calcd for C$_{20}$H$_{24}$NO$_4$S, 374.1426; found, 374.1428

General Procedure for the Synthesis of 16a–f (Method H). Exemplified for (*R*)-1-(3-(2-(Hydroxydiphenylmethyl)-pyrrolidin-1-ylsulfonyl)propyl)pyrimidine-2,4(1*H*,3*H*)-dione (16a). A suspension of **15e** (406 mg, 1.08 mmol), triphenylphosphine (567 mg, 2.16 mmol), and *N*-3-benzoyluracil (233 mg, 1.08 mmol) was added a toluene solution of diisopropyl azodicarboxylate (1.9 M, 1.14 mL, 2.16 mmol) at room temperature, the mixture was stirred at room temperature for 2 h. The reaction mixture was evaporated, and the residue was purified by a silica gel column chromatography (1–2% MeOH in CHCl$_3$) to give (*R*)-3-benzoyl-1-(3-(2-(hydroxydiphenyl-methyl)pyrrolidin-1-ylsulfonyl)propyl)pyrimidine-2,4(1*H*,3*H*)-dione as a mixture with triphenylphosphine oxide. The mixture was dissolved in a MeOH solution of methylamine (9.8 M, 4 mL) and stirred at room temperature for 1 h. The reaction mixture was evaporated, and the residue was purified by a silica gel column chromatography (2–4% MeOH in CHCl$_3$) to give **16a** (355 mg, 70% as a colorless foam). ^{1}H NMR (DMSO-*d$_6$*) δ 1.62–1.67 (3H, m), 1.81–1.84 (2H, m), 1.98–2.12 (2H, m), 2.35–2.40 (1H, m), 3.22–3.24 (1H, m), 3.40–3.64 (3H, m), 5.22 (1H, d, *J* = 6.2 Hz), 5.57 (1H, d, *J* = 7.6 Hz), 5.65 (1H, brs), 7.05–7.53 (11H, m), 11.3 (1H, brs). ^{13}C NMR (CDCl$_3$) δ 22.99, 26.00, 29.11, 47.25, 49.50, 50.64, 67.17, 81.17, 102.51, 126.68, 126.99, 127.35, 127.37, 128.17, 128.20, 144.11, 144.60, 145.76, 150.80, 163.37. Anal. Calcd for C$_{24}$H$_{27}$N$_3$O$_5$S·0.3H$_2$O: C, 60.69; H, 5.86; N, 8.85. Found: C, 60.40; H, 5.66; N, 8.71; [α]$^{25}_D$ = −13.14 (*c* 0.38, CHCl$_3$)

dUTPase Inhibition Assay. In vitro dUTPase inhibition assays were conducted by measuring the production of [5-^{3}H]dUMP from [5-^{3}H]dUTP. Briefly, 0.2 mL in total of a solution containing 0.02 mL of 1 μM dUTP (including 588 Bq/mL [5-^{3}H]dUTP), 0.05 mL of a 0.2 M Tris buffer solution (pH 7.4), 0.05 mL of 16 mM magnesium chloride, 0.02 mL of 20 mM 2-mercaptoethanol, 0.02 mL of a 1% aqueous solution of fetal bovine serum-derived albumin, 0.02 mL of varying concentrations of test compound solutions or pure water as a control, and 0.02 mL of a solution of human dUTPase was reacted at 37 °C for 15 min. After the reaction, the solution was immediately heated at 100 °C for 1 min to terminate the reaction followed by centrifugation at 15000 rpm for 2 min. An aliquot (150 μL) of the supernatant thus obtained by centrifugation was analyzed using an Atlantis dC18 column (manufactured by Waters Corp., 4.6 mm × 250 mm) and a high-performance liquid chromatograph (manufactured by Shimadzu Corp., Prominence). The inhibitory rate of the compound was calculated from the formula shown below. IC$_{50}$ (μM), the concentration of inhibitor yielding 50% inhibition rate, was obtained from concentration–inhibitory rate curve.

$$\text{Inhibitory rate(\%)} = [1 - (\text{amount of}[5\text{-}^3\text{H}]\text{dUMP}$$
$$\text{in presence of test solution(dpm)})$$
$$/(\text{amount of}[5\text{-}^3\text{H}]\text{dUMP as control(dpm)})] \times 100$$

Evaluation of in Vitro Cytotoxicity. HeLa S3 cells (human ovarian carcinoma) was grown in RPMI1640 medium supplemented with 10% fetal bovine serum (FBS). Exponentially growing cells were seeded in 96-well plates (1500 cells/0.18 mL) and incubated at 37 °C in a humidified 5% CO$_2$ atmosphere. After 24 h, various concentration of test compounds were added to the corresponding plates at a volume of 20 μL per well, and the plates were incubated for 72 h, and then cell proliferation was determined by the Crystal Violet assay. Optical density at 540 nm (OD$_{540}$) was measured by plate reader. Then, we calculated *T/C* (%) value, which was the ratio of OD$_{540}$ with drug treatment to without drug [*T/C* (%) = (OD$_{540}$ of treated well/OD$_{540}$ of nontreated well) × 100]. The EC$_{50}$ (μM) for the cytotoxicity of the

test compound was the concentration yielding 50% T/C value, which was calculated from concentration-T/C (%) curve.

Evaluation of the Enhancement of Growth Inhibition Activity of FdUrd in Vitro. HeLa S3 cells were seeded in 96-well plates (1500 cells/0.18 mL) and incubated at 37 °C in a humidified 5% CO_2 atmosphere as described above. After 24 h, five different concentration of test compounds and FdUrd (1 μM) were added to the corresponding plates at a volume of 20 μL per well. After 24 h incubation, thymidine (30 μM) was added to the plates at a volume of 10 μL per well. After further 48 h incubation, cell density was measured and T/C (%) values ware obtained as mentioned above. The EC_{50} for the enhancement of growth inhibition activity of FdUrd was calculated from the concentration-T/C (%) curve as a concentration at which the test compound reduced by half the T/C (%) value with the treatment of 1 μM FdUrd.

■ ASSOCIATED CONTENT

Ⓢ Supporting Information

Experimental details and analytical data for intermediates and test compounds except for the compounds described in the Experimental Section and details of ^{1}H NMR spectrum of **11s**, X-ray crystallography diffraction data and refinement statistics, and docking study of **16b** in the catalytic site of human dUTPase described in the manuscript. This material is available free of charge via the Internet at http://pubs.acs.org.

Accession Codes

PDB ID code of **16a** with human dUTPase: 3ARA.

■ AUTHOR INFORMATION

Corresponding Author

*Phone: 81-29-865-4527. Fax: 81-29-865-2170. E-mail: m-fukuoka@taiho.co.jp.

Notes

The authors declare no competing financial interest.

■ ACKNOWLEDGMENTS

■ ABBREVIATIONS USED

dUTPase, deoxyuridine triphosphatase; TS, thymidylate synthase; 5-FU, 5-fluorouracil; NTPs, nucleoside triphosphates; siRNA, small interfering RNA; Bn, benzyl; THF, tetrahydrofuran; EDC·HCl, N-(3-dimethylaminopropyl)-N'-ethylcarbodiimide hydrochloride; HOBt, 1-hydroxybenzotriazole; DMF, N,N-dimethylformamide; TEA, triethylamine; Bz, benzoyl; DIAD, diisopropyl azodicarboxylate; SAR, structure−activity relationship; NOE, nuclear Overhauser effect; clogP, calculated logP

■ REFERENCES

(1) Danneberg, P. B.; Montag, B. J.; Heidelberger, C. Studies on fluorinated pyrimidines. IV. Effects on nucleic acid metabolism in vivo. *Cancer Res.* **1958**, *18*, 329−334.

(2) Harrap, K. R.; Jackman, A. L.; Newell, D. R.; Taylor, G. A.; Hughes, L. R.; Calvert, A. H. Thymidylate synthase: a target for anticancer drug design. *Adv. Enzyme Regul.* **1989**, *29*, 161−179.

(3) Jackman, A. L.; Calvert, A. H. Folate-based thymidylate synthase inhibitors as anticancer drugs. *Ann. Oncol.* **1995**, *6*, 871−881.

(4) Jackman, A. L.; Kelland, L. R.; Kimbell, R.; Brown, M.; Gibson, W.; Aherne, G. W.; Hardcastle, A.; Boyle, F. T. Mechanisms of acquired resistance to the quinazoline thymidylate synthase inhibitor ZD1694 (Tomudex) in one mouse and three human cell lines. *Br. J. Cancer* **1995**, *71*, 914−924.

(5) Rhee, M. S.; Wang, Y.; Nair, M. G.; Galivan, J. Acquisition of resistance to antifolates caused by enhanced gamma-glutamyl hydrolase activity. *Cancer Res.* **1993**, *53*, 2227−2230.

(6) Salonga, D.; Danenberg, K. D.; Johnson, M.; Metzger, R.; Groshen, S.; Tsao-Wei, D. D.; Lenz, H. J.; Leichman, C. G.; Leichman, L.; Diasio, R. B.; Danenberg, P. V. Colorectal tumors responding to 5-fluorouracil have low gene expression levels of dihydropyrimidine dehydrogenase, thymidylate synthase, and thymidine phosphorylase. *Clin. Cancer Res.* **2000**, *6*, 1322−1327.

(7) Popat, S.; Matakidou, A.; Houlston, R. S. Thymidylate synthase expression and prognosis in colorectal cancer: a systematic review and meta-analysis. *J. Clin. Oncol.* **2004**, *22*, 529−536.

(8) Ladner, R. D.; Lynch, F. J.; Groshen, S.; Xiong, Y. P.; Sherrod, A.; Caradonna, S. J.; Stoehlmacher, J.; Lenz, H. J. dUTP nucleotidohydrolase isoform expression in normal and neoplastic tissues: association with survival and response to 5-fluorouracil in colorectal cancer. *Cancer Res.* **2000**, *60*, 3493−3503.

(9) Galperin, M. Y.; Moroz, O. V.; Wilson, K. S.; Murzin, A. G. House cleaning, a part of good housekeeping. *Mol. Microbiol.* **2006**, *59*, 5−19.

(10) Richardson, C. C.; Schildkraut, C. L.; Kornberg, A. Studies on the replication of DNA by DNA polymerases. *Cold Harbor Symp. Quantum Biol.* **1963**, *28*, 9−19.

(11) Longley, D. B.; Harkin, D. P.; Johnston, P. G. 5-Fluorouracil: mechanisms of action and clinical strategies. *Nature Rev. Cancer* **2003**, *3*, 330−338.

(12) Curtin, N. J.; Harris, A. L.; Aherne, G. W. Mechanism of cell death following thymidylate synthase inhibition: 2′-deoxyuridine-5′-triphosphate accumulation, DNA damage, and growth inhibition following exposure to CB3717 and dipyridamole. *Cancer Res.* **1991**, *51*, 2346−2352.

(13) Webley, S. D.; Hardcastle, A.; Ladner, R. D.; Jackman, A. L.; Aherne, G. W. Deoxyuridine triphosphatase (dUTPase) expression and sensitivity to the thymidylate synthase (TS) inhibitor ZD9331. *Br. J. Cancer* **2000**, *83*, 792−799.

(14) Mol, C. D.; Harris, J. M.; McIntosh, E. M.; Tainer, J. A. Human dUTP pyrophosphatase: uracil recognition by a beta hairpin and active sites formed by three separate subunits. *Structure* **1996**, *4*, 1077−1092.

(15) Bertani, L. E.; Haeggmark, A.; Reichard, P. Enzymatic synthesis of deoxyribonucleotides. II. Formation and interconversion of deoxyuridine phosphates. *J. Biol. Chem.* **1963**, *238*, 3407−3413.

(16) Grindey, G. R.; Nichol, C. A. Mammalian deoxyuridine 5′-triphosphate pyrophosphatase. *Biochim. Biophys. Acta* **1971**, *240*, 180−183.

(17) McIntosh, E. M.; Haynes, R. H. dUTP pyrophosphatase as a potential target for chemotherapeutic drug development. *Acta Biochim. Pol.* **1997**, *44*, 159−171.

(18) Caradonna, S. J.; Cheng, Y. C. The role of deoxyuridine triphosphate nucleotidohydrolase, uracil-DNA glycosylase, and DNA polymerase alpha in the metabolism of FUdR in human tumor cells. *Mol. Pharmacol.* **1980**, *18*, 513−520.

(19) An, Q.; Robins, P.; Lindahl, T.; Barnes, D. E. 5-Fluorouracil incorporated into DNA is excised by the Smug1 DNA glycosylase to reduce drug cytotoxicity. *Cancer Res.* **2007**, *67*, 940−945.

(20) Wilson, P. M.; Fazzone, W.; LaBonte, M. J.; Deng, J.; Neamati, N.; Ladner, R. D. Novel opportunities for thymidylate metabolism as a therapeutic target. *Mol. Cancer Ther.* **2008**, *7*, 3029−3037.

(21) Ingraham, H. A.; Tseng, B. Y.; Goulian, M. Nucleotide levels and incorporation of 5-fluorouracil and uracil into DNA of cells treated with 5-fluorodeoxyuridine. *Mol. Pharmacol.* **1982**, *21*, 211−216.

(22) Koehler, S. E.; Ladner, R. D. Small interfering RNA-mediated suppression of dUTPase sensitizes cancer cell lines to thymidylate synthase inhibition. *Mol. Pharmacol.* **2004**, *66*, 620−626.

(23) Takatori, H.; Yamashita, T.; Honda, M.; Nishino, R.; Arai, K.; Takamura, H.; Ohta, T.; Zen, Y.; Kaneko, S. dUTP pyrophosphatase expression correlates with a poor prognosis in hepatocellular carcinoma. *Liver Int.* **2010**, *30*, 438−446.

(24) Kawahara, A.; Akagi, Y.; Hattori, S.; Mizobe, T.; Shirouzu, K.; Ono, M.; Yanagawa, T.; Kuwano, M.; Kage, M. Higher expression of deoxyuridine triphosphatase (dUTPase) may predict the metastasis potential of colorectal cancer. *J. Clin. Pathol.* **2009**, *62*, 364−369.

(25) Zalud, P.; Wachs, W. O.; Nyman, P. O.; Zeppezauer, M. M. Inhibition of the proliferation of human cancer cells in vitro by substrate-analogous inhibitors of dUTPase. *Adv. Exp. Med. Biol.* **1994**, *370*, 135−138.

(26) Persson, T.; Larsson, G.; Nyman, P. O. Synthesis of 2′-deoxyuridine 5′-(alpha,beta-imido) triphosphate: a substrate analogue and potent inhibitor of dUTPase. *Bioorg. Med. Chem.* **1996**, *4*, 553−556.

(27) Nguyen, C.; Kasinathan, G.; Leal-Cortijo, I.; Musso-Buendia, A.; Kaiser, M.; Brun, R.; Ruiz-Perez, L. M.; Johansson, N. G.; Gonzalez-Pacanowska, D.; Gilbert, I. H. Deoxyuridine triphosphate nucleotido-hydrolase as a potential antiparasitic drug target. *J. Med. Chem.* **2005**, *48*, 5942−5954.

(28) Whittingham, J. L.; Leal, I.; Nguyen, C.; Kasinathan, G.; Bell, E.; Jones, A. F.; Berry, C.; Benito, A.; Turkenburg, J. P.; Dodson, E. J.; Ruiz Perez, L. M.; Wilkinson, A. J.; Johansson, N. G.; Brun, R.; Gilbert, I. H.; Gonzalez Pacanowska, D.; Wilson, K. S. dUTPase as a platform for antimalarial drug design: structural basis for the selectivity of a class of nucleoside inhibitors. *Structure* **2005**, *13*, 329−338.

(29) Nguyen, C.; Ruda, G. F.; Schipani, A.; Kasinathan, G.; Leal, I.; Musso-Buendia, A.; Kaiser, M.; Brun, R.; Ruiz-Perez, L. M.; Sahlberg, B. L.; Johansson, N. G.; Gonzalez-Pacanowska, D.; Gilbert, I. H. Acyclic nucleoside analogues as inhibitors of *Plasmodium falciparum* dUTPase. *J. Med. Chem.* **2006**, *49*, 4183−4195.

(30) Jiang, Y. L.; Chung, S.; Krosky, D. J.; Stivers, J. T. Synthesis and high-throughput evaluation of triskelion uracil libraries for inhibition of human dUTPase and UNG2. *Bioorg. Med. Chem.* **2006**, *14*, 5666−5672.

(31) Mc Carthy, O. K.; Schipani, A.; Buendia, A. M.; Ruiz-Perez, L. M.; Kaiser, M.; Brun, R.; Pacanowska, D. G.; Gilbert, I. H. Design, synthesis and evaluation of novel uracil amino acid conjugates for the inhibition of *Trypanosoma cruzi* dUTPase. *Bioorg. Med. Chem. Lett.* **2006**, *16*, 3809−3812.

(32) Beck, W. R.; Wright, G. E.; Nusbaum, N. J.; Chang, J. D.; Isselbacher, E. M. Enhancement of methotrexate cytotoxicity by uracil analogues that inhibit deoxyuridine triphosphate nucleotidohydrolase (dUTPase) activity. *Adv. Exp. Med. Biol.* **1986**, *195B*, 97−104.

(33) Marriott, J. H.; Aherne, G. W.; Hardcastle, A.; Jarman, M. Synthesis of certain 2′-deoxyuridine derivatives containing substituted phenoxy groups attached to C-5′; evaluation as potential dUTP analogues. *Nucleosides, Nucleotides Nucleic Acids* **2001**, *20*, 1691−1704.

(34) Hampton, S. E.; Baragana, B.; Schipani, A.; Bosch-Navarrete, C.; Musso-Buendia, J. A.; Recio, E.; Kaiser, M.; Whittingham, J. L.; Roberts, S. M.; Shevtsov, M.; Brannigan, J. A.; Kahnberg, P.; Brun, R.; Wilson, K. S.; Gonzalez-Pacanowska, D.; Johansson, N. G.; Gilbert, I. H. Design, synthesis, and evaluation of 5′-diphenyl nucleoside analogues as inhibitors of the *Plasmodium falciparum* dUTPase. *ChemMedChem* **2011**, *6*, 1816−1831.

(35) Li, K.; Zhou, Z.; Wang, L.; Chen, Q.; Zhao, G.; Zhou, Q.; Tang, C. Asymmetric carbonyl reduction with borane catalyzed by chiral phosphinamides derived from L-amino acid. *Tetrahedron: Assymmetry* **2003**, *14*, 95−100.

(36) Keuser, C.; Pindur, U. Oligopyrrole carboxamides linked with a nucleobase as potential DNA minor groove binding ligands: synthesis, DNA binding and biological evaluation. *Pharmazie* **2006**, *61*, 261−268.

(37) Ahn, H.; Choi, T. H.; De Castro, K.; Lee, K. C.; Kim, B.; Moon, B. S.; Hong, S. H.; Lee, J. C.; Chun, K. S.; Cheon, G. J.; Lim, S. M.; An, G. I.; Rhee, H. Synthesis and evaluation of *cis*-1-[4-(hydroxymethyl)-2-cyclopenten-1-yl]-5-[(124)I]iodouracil: a new potential PET imaging agent for HSV1-tk expression. *J. Med. Chem.* **2007**, *50*, 6032−6038.

(38) Lipinsky, C. A.; Lombardo, F.; Dominy, B. W.; Feeney, P. J. Experimental and computational approaches to estimate solubility and permeability in drug discovery and development setting. *Adv. Drug Delivery Rev.* **1997**, *23*, 3−25.

(39) Varga, B.; Barabas, O.; Kovari, J.; Toth, J.; Hunyadi-Gulyas, E.; Klement, E.; Medzihradszky, K. F.; Tolgyesi, F.; Fidy, J.; Vertessy, B. G. Active site closure facilitates juxtaposition of reactant atoms for initiation of catalysis by human dUTPase. *FEBS Lett.* **2007**, *581*, 4783−4788.

(40) Fernandez, A.; Scott, R. Dehydron: a structurally encoded signal for protein interaction. *Biophys. J.* **2003**, *85*, 1914−1928.

(41) Fernandez, A.; Maddipati, S. A priori inference of cross reactivity for drug-targeted kinases. *J. Med. Chem.* **2006**, *49*, 3092−3100.

(42) Fernandez, A.; Sanguino, A.; Peng, Z.; Ozturk, E.; Chen, J.; Crespo, A.; Wulf, S.; Shavrin, A.; Qin, C.; Ma, J.; Trent, J.; Lin, Y.; Han, H. D.; Mangala, L. S.; Bankson, J. A.; Gelovani, J.; Samarel, A.; Bornmann, W.; Sood, A. K.; Lopez-Berestein, G. An anticancer C-Kit kinase inhibitor is reengineered to make it more active and less cardiotoxic. *J. Clin. Invest.* **2007**, *117*, 4044−4054.